RSC Advances

PAPER

View Article Online
View Journal | View Issue

Cite this: *RSC Adv.*, 2020, **10**, 26120

Guiding neural extensions of PC12 cells on carbon nanotube tracks dielectrophoretically formed in poly(ethylene glycol) dimethacrylate

Fikri Seven,[a] Tansu Gölcez,[a] Ziyşan Buse Yaralı,[b] Günnur Onak,[b] Ozan Karaman[c] and Mustafa Şen *[c]

Received 20th May 2020
Accepted 4th July 2020

DOI: 10.1039/d0ra04496b

rsc.li/rsc-advances

The PC12 cell line has been widely used as an *in vitro* model for studying neuronal differentiation and identifying the factors affecting the process. It has the ability to differentiate in the presence of nerve growth factor (NGF), resulting in neural extensions called dendrites and axons. In this study, first the impact of randomly distributed multi-walled carbon nanotubes (MWCNTs) in poly(ethylene glycol) dimethacrylate (PEGDMA) on PC12 cell differentiation was investigated in terms of neurite length, number of neurite per cell and differentiation marker gene expression profile. Then, dielectrophoretically aligned MWCNTs in PEGDMA was used to guide and support the neuronal differentiation of PC12 cells in the presence of NGF. The method is expected to be useful in revealing the nanotopographical role in fundamental studies and understanding of nanotopographical effects for biomedical applications on nerve regeneration.

1. Introduction

There are millions of people worldwide experiencing some degree of nerve injury, mostly caused by traumatic events and diseases.[1,2] Even though neurons have some degree of ability to regenerate, functional recovery is usually limited without structural support. The local microenvironment has a profound effect on the regulation of cell adhesion, proliferation and differentiation. The establishment of functional nervous system requires guided neurite outgrowth, a process in which growing neurons produce connections *via* extensions.[3,4] Tissue engineering offers promising approaches for designing scaffolds with proper cues and properties for the development of neuronal circuits and induction of neuronal regeneration after injury.[5,6] Developing *in vitro* models using tissue engineering techniques can be useful in a variety of ways, from understanding the regulatory mechanisms of neurite outgrowth to identifying possible drugs that could mitigate barriers to nervous system regeneration.[7] Understanding the regulatory mechanism of neurite outgrowth is crucial not only in understanding brain development but also in finding new ways to induce neurite re-outgrowth in patients with neurodegenerative diseases.[8] Clements *et al.* used tubular channels enhanced with aligned nanofiber-based thin films to modulate endogenous nerve repair processes.[9] They showed that regeneration across critically sized nerve gaps may be significantly enhanced by a guidance channel provided by minimal topographic cues. The potential of biodegradable and biocompatible polyethyleneglycol (PEG) hydrogels and their composites has been investigated for neural degenerative diseases.[10–13] Guarino *et al.* demonstrated that macroporous polyaniline (PANi) and polyethyleneglycol diacrylate (PEGDA) hybrid gels present proper electrical and morphological properties in driving nerve cells in regenerative processes.[14] Shah *et al.* developed a biocompatible hydrogel by entrapping carbon nanotubes (CNTs) into PEG during gelation.[15] The CNTs enhanced the conductivity of the hydrogel and provided sites for cell attachment, resulting in higher PC12 cell viability as compared to PEG hydrogel. The positive impact of electrical stimulation on neuronal differentiation has been demonstrated with conductive PEG hydrogels in the presence of nerve growth factors (NGF) by several groups.[16,17] Dielectrophoresis (DEP) is described as the movement of dielectric particles under the effect of a non-uniform electric field. Using dielectrophoresis to align CNTs in a hydrogel has been demonstrated by Azcón *et al.*[18] Aligned CNTs improved electrical and mechanical properties of the hydrogel, resulting in myofibers with more maturation and contractility after electrical stimulation. In the present study, the impact of randomly distributed multi-walled CNTs (MWCNT) in poly(ethylene glycol) dimethacrylate (PEGDMA) on PC12 cell differentiation was first investigated in terms of neurite length, number of neurite per cell and differentiation marker gene expression profile. Then, DEP was used to fabricate PEGDMA with aligned CNTs to guide and support the neuronal differentiation of PC12 cells in the presence

[a]*Izmir Katip Celebi University, Graduate School of Natural and Applied Sciences, Department of Biomedical Technologies/Master of Science, Izmir, Turkey*
[b]*Izmir Katip Celebi University, Graduate School of Natural and Applied Sciences, Biomedical Test, Calibration, Application and Research Center, Izmir, Turkey*
[c]*Izmir Katip Celebi University, Faculty of Engineering and Architecture, Biomedical Engineering, Izmir, Turkey. E-mail: mustafa.sen@ikc.edu.tr*

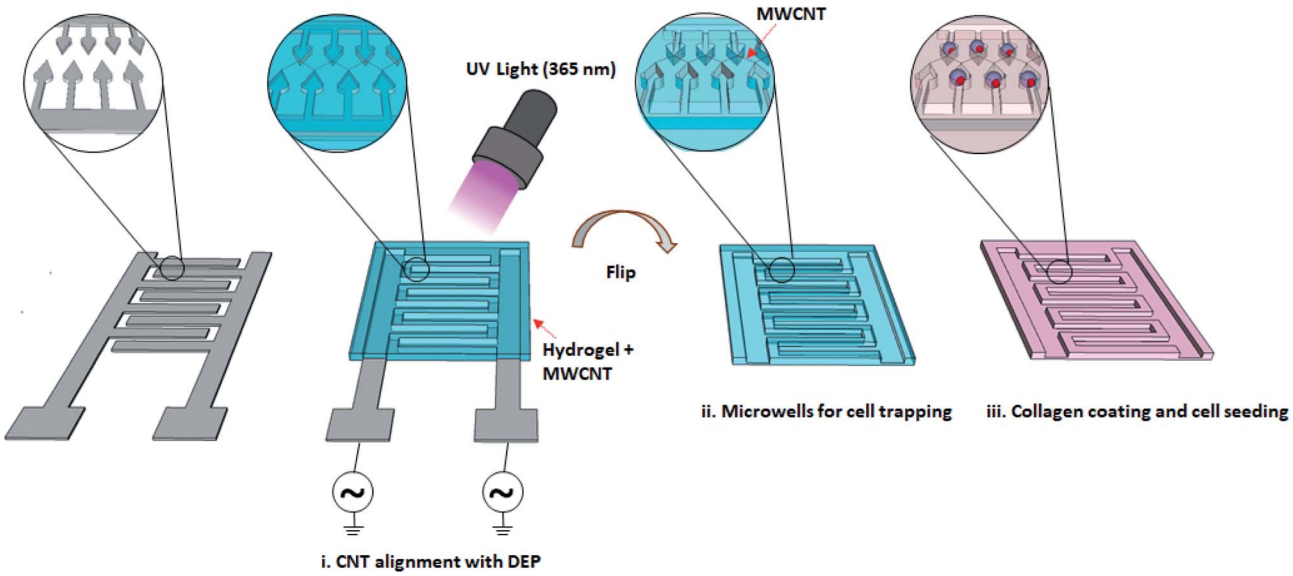

Fig. 1 A schematic illustration of the strategy used to align and fix MWCNTs in PEGDMA. CNTs were aligned in PEGDMA on an IDA chip using DEP and then fixed *via* UV crosslinking. The gel with aligned CNTs was peeled off, flipped and placed in a culture dish. After coating the entire surface with collagen, PC12 cells were seeded on the gel and cultured for 24 h at 37 °C. The next day, NGF was added to the medium to induce neuronal differentiation.

of NGF (Fig. 1). The results could have a great potential for guiding neural outgrowth and producing neuronal circuits for various applications ranging from nerve regeneration to drug discovery.

2. Materials and methods

2.1. Materials

Collagen (type IV, 0.5–2 mg ml^{-1}) (Sigma-Aldrich, USA), acetic acid (Sigma-Aldrich, USA), trypsin (Gibco, USA), donor horse serum (DHS) (Capricorn, Germany), fetal bovine serum (FBS) (Sigma-Aldrich, USA), L-glutamine (Gibco, USA), gentamicin (Gibco, USA), RPMI-1640 (Sigma-Aldrich, USA), nerve growth factor (NGF) (Vipera lebetina venom) (Sigma-Aldrich, USA), phosphate-buffered saline (PBS) (Sigma Aldrich, USA), NaOH (Sigma-Aldrich, USA), Irgacure (Sigma-Aldrich, USA), PEGDMA (PolyScience, USA), MWCNTs (Nanografi, Turkey), 3-(trimethoxysilyl)propyl methacrylate (TMSPM) (Sigma-Aldrich, USA), AZ5214E (MicroChemicals, Germany), Calcein-AM Cell Viability Assay Kit (Biotium, USA), Blood/Cell Total RNA Mini Kit (Geneaid, Sijhih City, Taiwan), M-MuLV First Strand cDNA Synthesis Kit (Biomatik, Ontario, Canada).

2.2. Fabrication of the chip

A gold-coated glass slide was first treated with air plasma to remove organic residues on the surface. Subsequently, a reversal photoresist (AZ5214E) was spun coated on the glass-slide at 2000 rpm for 1 min and baked at 90 °C for 30 min. The photoresist was UV irradiated through a chromium mask with the desired patterns and developed using a NaOH-based developer solution. The Au film in exposed areas were then removed by ion beam etching and the remaining photoresist was removed using acetone.

2.3. Cell culture and staining

PC12 cells were purchased from DSMZ (Braunschweig, Germany) and cultured in RPMI-1640 containing 10% DHS, 1% FBS, 1% L-glutamine and 0.1% gentamicin at 37 °C under a 5% CO_2 humidified atmosphere. Cells were cultured in collagen coated flasks to facilitate adherent cell growth and the culture medium was refreshed every two days. For neuronal cell differentiation, the culture medium was refreshed with NGF-containing (100 ng ml^{-1}) culture medium every two days. Calcein-AM Cell Viability Assay Kit was used to image cells with a fluorescent microscopy. Briefly, cell were washed twice with PBS and incubated in a PBS solution containing 2 μL calcein-AM and 4 μL EthD-1 (Ethidium Homodimer-1) for 60 min in dark. Subsequently, the stained cells were washed twice with PBS and imaged using a fluorescence microscopy (Axio Vert.A1, Zeiss, Germany).

2.4. Fabrication of PEGDMA hydrogels with no, randomly distributed and aligned CNTs

A prepolymer was prepared by dissolving 10% PEGDMA + 1% Irgacure in ultra-pure water using ultrasonic bath. MWCNTs were washed three-times with ultra-pure water by centrifugation (17 000 rpm, 30 min). Next, a prepolymer with 0.3 mg ml^{-1} MWCNT was prepared. For the fabrication of PEGDMA with no and randomly distributed CNTs, a glass slide was treated with air plasma and then methacrylated with TMSPM under vacuum for 1 h. A PET film spacer (thickness, 1 mm) was placed between the surface modified and an unmodified glass-slide to form a chamber, which was then filled with either PEGDMA or

MWCNT-PEGDMA prepolymer. Each prepolymer was polymerized with UV light (7 mW cm^{-2}) for 3 min. As for the PEGDMA with aligned CNTs, the chamber was formed between the TMSPM surface modified glass-slide and an Au-IDA, which was then filled with the MWCNT-PEGDMA pre-polymer. A sinusoidal AC voltage of 10 Vpp with identical frequency (1 MHz) and opposite phase was applied to the two microband arrays of the Au-IDA using a waveform generator (33500B, Keysight, USA) to create a nonuniform electric field for the alignment the CNTs. After 1 min, the PEGDMA prepolymer was polymerized the same way as described above.

2.5. Electrical properties of PEGDMA and the hybrid hydrogels

First, the current–voltage (*I–V*) curves of PEGDMA, PEGDMA with randomly distributed CNTs and PEGDMA with dielectrophoretically aligned CNTs were obtained using the two-probes of a source/measure unit (B2902A, Keysight, ABD) connected to a computer. The measurement was performed in a Faraday cage at room temperature to reduce noise. The voltage was swept between −2 and 2 V at a scan rate of 0.1 V and the resulting current was recorded. All the hydrogels were formed on Au-IDA chips and the measurements were conducted using the connection pads of the chips. Next, electrochemical impedance spectroscopy (EIS) measurements were performed for the same test groups using an Autolab PGSTAT204 potentiostat (Metrohm, Netherlands). The data were monitored and analyzed using Autolab Nova software. Impedance spectra of all the samples were recorded on the Au-IDA chips over a frequency range of 1 to 100 Hz with a 25 mV perturbation amplitude.

2.6. Neural differentiation of PC12 on PEGDMA and the hybrid hydrogels

After polymerization, the surface modified glass-slide with PEGDMA or hybrid hydrogels was detached and placed in a culture dish with the hydrogel on top. The whole surface of the hydrogels was coated with collagen (type IV, 0.5–2 mg ml^{-1}) for PC12 cell attachment and spreading. PC12 cells were seeded on the gel with a cell density of 5000 cells per cm^2 and cultured in RPMI 1640 supplemented with 10% DHS, 1% FBS, 1% L-glutamine and 0.1% gentamicin for 24 h at 37 °C. The next day, the medium was changed to a fresh culture medium containing 100 ng ml^{-1} NGF to induce cell differentiation. The medium with NGF was changed once every 2 days.

2.7. Real-time qPCR

Following 6 days of differentiation, total cellular RNA was isolated using Blood/Cell Total RNA Mini Kit. The extracted RNA was converted to cDNA using M-MuLV First Strand cDNA Synthesis Kit. The cDNA obtained was used for RT-qPCR (Step One Plus Real-time PCR system, Applied Biosystems, Foster City, USA) with appropriate gene-specific primers. All primer sets (GAPDH, synapsin-1 and GAP43) were purchased from Atlas Biotechnology Turkey and validated for qPCR. The forward and reverse primer sequences are as follows; GAPDH: 5′-TGGCGCTGAGTACGTCGTG-3′/5′-ATGGCATGGACTGTGGTCAT-3′, GAP43: 5′-AGAAAGCAGCCA AGCTGAGGAGG-3′/5′-CAGGAGAGACAGGGTTCAGGTGG-3′ and synapsin-1: 5′-CAGGGTCAAGGCCGCCAGTC-3′/5′-CACAT CCTGGCTGGGTTTCTG-3′. The differential expression of the genes was quantified by StepOne Software v2.3 and normalized against that of the GAPDH gene. The gene expression analysis was repeated at least three times for each sample.

2.8. Statistical analysis

All numerical data given in gene expression and average neurite length analysis were presented as mean ± SEM for $n \geq 3$. Data analysis and histograms were obtained using Microsoft-Excel 2013 software. The significant differences among groups were computed by two-tailed Student's *t*-test. Statistical difference was considered significant when $p < 0.05$.

3. Results and discussion

First the differentiation behavior of PC12 cells was investigated on PEGDMA with randomly distributed MWCNTs in comparison to PEGDMA hydrogel. The cells were seeded and allowed to differentiate on a flat surface which was achieved by polymerizing the hydrogel in a chamber formed between two glass slides. A glass slide surface was modified with TMSPM to facilitate the covalent binding of the hydrogel to the glass slide, which was necessary to culture cells on the hydrogel for a long time without detachment. Since PC12 cells need a surface modified with various biochemical cues such as poly-L-lysine, laminin, fibronectin and collagen for an improved cell attachment, the surface of the hydrogel was coated with collagen (type IV) prior to cell seeding. After 6 days of differentiation, PC12 cells were analyzed in terms of distribution of neurite length, number of neurites per cell and average neurite length. The optical images showed that PC12 cell neurite extensions were predominantly longer on MWCNT-PEGDMA hybrid hydrogels compared to PEGDMA (Fig. $2a_{i\ and\ ii}$). The histogram of neurite length and number of neurite per cell (Fig. $2b_{i\ and\ ii}$) clearly showed very different patterns for the two hydrogels. An average neurite length for each group was calculated by taking the longest 50 neurites into account and it appeared that the average neurite length for PC12 cells grown on PEGDMA (108.23 ± 37.02 μm) was significantly lower than those grown on MWCNT-PEGDMA (196.98 ± 31.83 μm) (Fig. $2b_{iii}$). These two hydrogels were also compared based on gene expression profile of two differentiation markers; synapsin-1 and GAP-43. Synapsin-1 is required for synapse formation, whereas GAP-43 is considered a marker for axon re-generation.[19,20] The expression levels of genes were normalized with respect to the internal reference gene GAPDH. Fig. 2c clearly showed that the expression of the two markers increased significantly on the hybrid hydrogel as compared to PEGDMA in the presence of NGF. Altogether, the results clearly showed that MWCNT-PEGDMA presented a better surface and microenvironment for the differentiation of PC12 cells. In other words, CNTs had a profound effect on neurite outgrowth by providing nano-topographical cues.

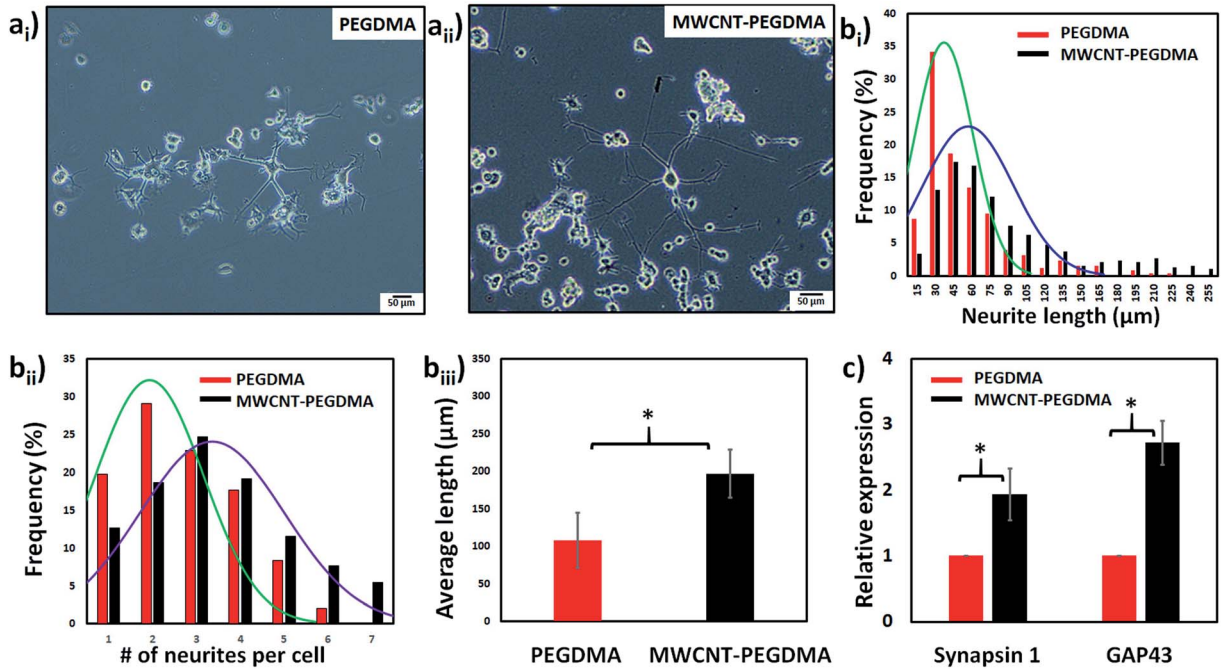

Fig. 2 Optic images of PC12 cells cultured for 7 d on PEGDMA (a_i) and MWCNT-PEGDMA (random) (a_{ii}), respectively. The cells were then analyzed in terms of distribution of neurite length (b_i), number of neurites per cell (b_{ii}) and average neurite length (b_{iii}). The expression of neuronal markers synapsin 1 and GAP-43 was also performed at day 7 using real-time PCR (c) (*$p < 0.05$).

After confirming the positive impact of CNTs on PC12 differentiation, dielectrophoresis (DEP) was employed on an Au-interdigitated electrode array (IDA) microchip to align CNTs (MWCNTs) in PEGDMA hydrogels for guidance and support of PC12 neural differentiation in the presence of NGF. Controlling neuronal outgrowth is a key process for constructing a functional neuronal circuit and neuronal regeneration following a nerve injury. An Au-IDA chip with electrodes shaped in triangles and crenellated was used to align and fix MWCNTs in PEGDMA (Fig. 1) in a zig-zag shape.[21–23] Prior to cell experiment, the DC conductivity of PEGDMA with aligned CNTs was obtained using a source/measure unit and compared to those of PEGDMA with no and randomly distributed CNTs. As can be seen in Fig. 3a, aligned CNT tracks drastically improved the conductivity of PEGDMA. When +2.0 V was applied, the electrical currents measured from PEGDMA with no, randomly distributed and aligned CNTs were 1.57, 6.58 and 24.2 μA, respectively. The improved conductivity in aligned CNT tracks that led to higher electrical current was caused by the formation of interlinked network of CNTs following DEP. A similar trend was observed in impedance analysis which was obtained in the frequency range of 1 to 100 Hz with a 25 mV perturbation amplitude (Fig. 3b). The electrical impedances of PEGDMA with no, randomly distributed and aligned CNTs at 1 Hz were

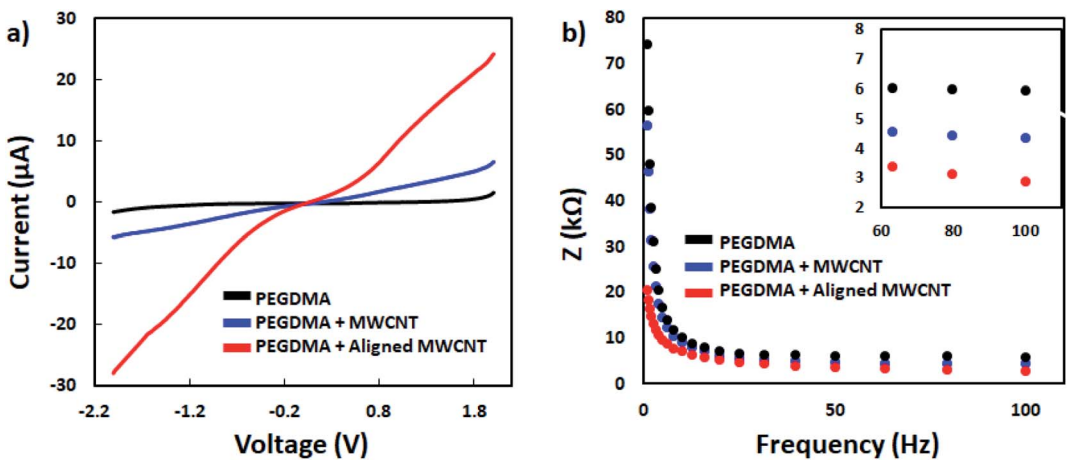

Fig. 3 *I–V* curves (a) and impedance measurement results (b) of PEGDMA with no, random and aligned CNTs.

measured as 74.31, 56.43 and 20.64 kΩ, respectively. Next, the hybrid hydrogel with aligned CNTs was detached from the DEP device for the cell experiment and placed in a culture dish with the hydrogel on top. Here, the hydrogel became covalently linked to the glass slide due to the surface modification with TMSPM. An AFM analysis showed that the Au electrodes had a thickness around 0.39 μm (Fig. 4a). Since, the micropatterns were transferred to the hybrid hydrogel after UV irradiation, it was assumed that the micropatterns in the hydrogels had a similar thickness which somehow mitigated the placement of PC12 cells close to aligned CNT tracks as shown in Fig. 4b. PC12 cells were allowed to differentiate on the hydrogel with aligned CNTs for 6 days prior to imaging. Since the aligned CNTs were not transparent, the calcein AM dye was used to stain PC12 cells and thus, image their extensions on these tracks (Fig. 4c$_{i-iii}$). Aligned CNTs mediated the guidance of neural extensions (Fig. 4c$_i$) and thus connecting PC12 cells to each other (Fig. 4c$_{ii}$). Fig. 4c$_{ii}$ clearly shows that CNT tracks had a good performance in directing the neural outgrowth as extensions of both cells grew in two directions along the CNT tracks. In Fig. 4c$_{iii}$, the extension of a PC12 cell had an approximately 37° deflection from the original trajectory when the extension reached a CNT track, in which case the CNT track successfully directed the extension of the cell to a different path. In addition, cells that have both at least one visible neural extension and in contact with CNT tracks ($n = 156$) were analyzed to demonstrate the performance of CNT tracks in directing neurites (Fig. 4d). According to the results, 87.82% of the cells had at least one neural extension guided by the CNT tracks; 59.62% of the cells had one and 28.20% of the cells had two neural extensions guided by the CNT tracks. 12.18% of the cells had at least one neural extension but no apparent one guided by the CNT tracks.

Physical signal received by local contact guidance along with molecular stimuli govern the fate of neuronal differentiation.[24] Various reports emphasize that surface topography provides a molecular pathway for controlling the directional growth and polarity of differentiating neurons.[25,26] It can be used to control cell fate in regenerative medicine. Following the establishment and maturation of focal adhesions, developing neural extensions check the surrounding environment to determine the way to the final target, a process known as neurite path-finding.[27] Basically, path-finding behavior and neural outgrowth of neurons are governed by filopodia and lamellipodia and the dynamic stability of the two determines the response to nano-topographical cues.[28] Here, many single CNTs were brought together by dielectric force to form CNT tracks in a hydrogel. These tracks basically provided instructive physical cues for the two actin-based molecular structures in developing neurites to recognize, which resulted in modulation of neurite path-finding and thus guidance of the neural outgrowth of PC12 cells. Even though hydrogels have been used for building neuronal networks, aligned CNTs have given the hydrogel more control over the guidance of neuronal extensions.[29] In addition, the approach presented here offers neuronal guidance in an open environment which provides a better diffusion for the nutrients and the growth factors (present or secreted by the cells) than solid channels.[30] *In vitro* functional neuronal networks with well-defined topology have a great potential in drug discovery and elucidating the causes of neurological diseases. It can also be applied to building patient-specific disease model chips.[31] Since more complex CNT networks can be formed by just changing the electrode design as demonstrated before,[23] the proposed approach has the capacity for building well-defined neuronal networks with controlled topology.

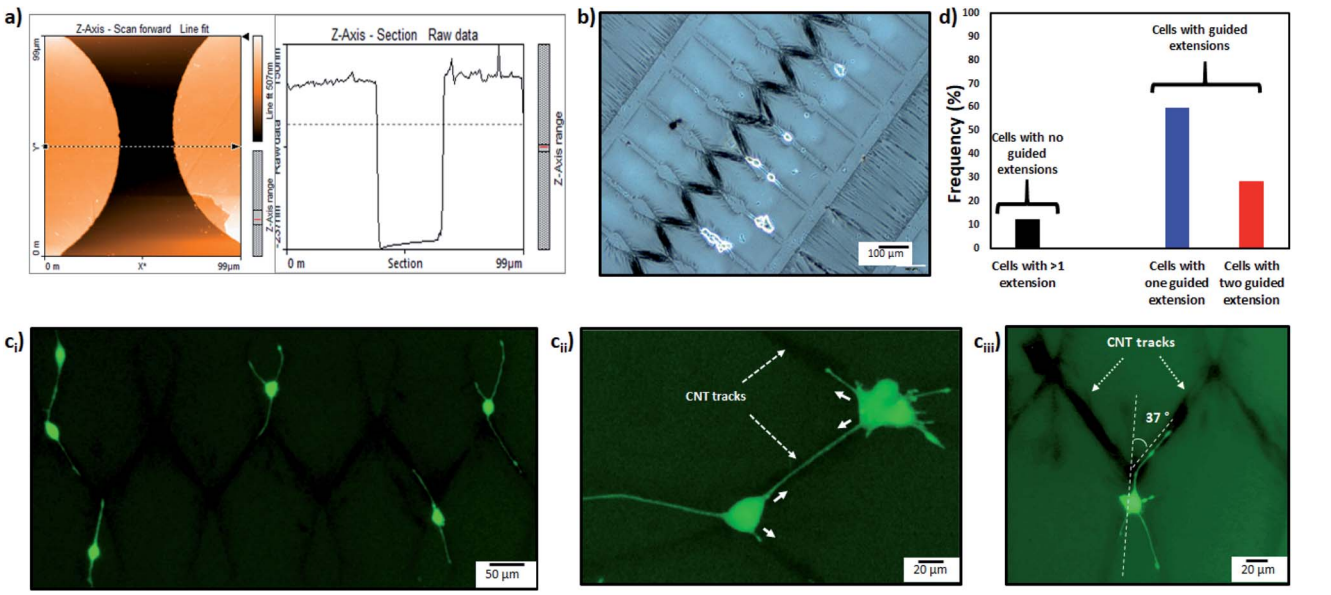

Fig. 4 AFM was used to determine the height of electrodes and thus the depth of micropatterns in PEGDMA hydrogels (a). The micropatterns helped in entrapping cells and keeping them close to aligned CNTs (CNT tracks) (b). The CNT tracks mediated the guidance of neural extensions (c$_i$) and thus connecting PC12 cells to each other (c$_{ii}$). A clear deflection in neural extension can be observed when the extension reached a CNT track (c$_{iii}$). Frequency of cells with extensions guided by CNT tracks (d).

4. Conclusion

Here, the positive impact of CNTs on PC12 differentiation was first investigated with respect to cell morphology and expression of neural differentiation markers, and then CNT tracks were dielectrophoretically formed in PEGDMA hydrogels to demonstrate their ability in guidance of neural extensions. In summary, PC12 cells differentiated significantly better on PEGDMA with randomly distributed CNTs than PEGDMA alone, which can be attributed to nanotopographical cues and higher conductivity provided by the CNTs. A microenvironment consisting of micropatterns and CNT tracks was created using an Au-IDA and DEP. It allowed roughly positioning of PC12 cells and guidance of neural outgrowth. Since the effect of nanotopographical cues on the growth of axon and dendrites is still elusive, the proposed method could be useful for revealing the nanotopographical role in fundamental studies. It could also contribute to understanding of nanotopographical effects for biomedical applications where nerve regeneration from a position to a predefined direction is required. It is now planned to coat only CNTs with collagen to limit the growth of PC12 cells on CNTs and guide their extensions. New electrode designs will be used to form complex neuronal circuits.

Conflicts of interest

There are no conflicts to declare.

Acknowledgements

This research was supported by the Scientific and Technological Research Council of Turkey (TUBITAK) (Project No: 215E003).

References

1 M. Imaninezhad, K. Pemberton, F. Xu, K. Kalinowski, R. Bera and S. P. Zustiak, *J. Neural Eng.*, 2018, **15**, 056034.
2 J. Noble, C. A. Munro, V. S. Prasad and R. Midha, *J. Trauma*, 1998, **45**, 116–122.
3 S. Millecamps and J.-P. Julien, *Nat. Rev. Neurosci.*, 2013, **14**, 161–176.
4 Y.-N. Jan and L. Y. Jan, *Neuron*, 2003, **40**, 229–242.
5 K. M. Dang, P. Rinklin, J. Schnitker, B. Haberkorn, K. Zobel, S. Gribaudo, A. L. Perrier, J. Carolus, M. Daenen, S. Weigel, H. Luksch, A. Offenhäusser and B. Wolfrum, *Phys. Status Solidi A*, 2017, **214**, 1600729.
6 O. V. Cangellaris and M. U. Gillette, *Front. Mater.*, 2018, **5**, 21.
7 W. Belkaid, P. Thostrup, P. T. Yam, C. A. Juzwik, E. S. Ruthazer, A. S. Dhaunchak and D. R. Colman, *BMC Biotechnol.*, 2013, **13**, 86.
8 W. Li, W. W. R. Chan, J. C. K. Ngo and K.-F. Lau, *Neural Regener. Res.*, 2018, **13**, 2085.
9 I. P. Clements, Y.-T. Kim, A. W. English, X. Lu, A. Chung and R. V. Bellamkonda, *Biomaterials*, 2009, **30**, 3834–3846.
10 M. J. Mahoney and K. S. Anseth, *Biomaterials*, 2006, **27**, 2265–2274.
11 S. Royce Hynes, L. M. McGregor, M. Ford Rauch and E. B. Lavik, *J. Biomater. Sci., Polym. Ed.*, 2007, **18**, 1017–1030.
12 S. R. Hynes, M. F. Rauch, J. P. Bertram and E. B. Lavik, *J. Biomed. Mater. Res., Part A*, 2009, **89**, 499–509.
13 U. Freudenberg, A. Hermann, P. B. Welzel, K. Stirl, S. C. Schwarz, M. Grimmer, A. Zieris, W. Panyanuwat, S. Zschoche, D. Meinhold, A. Storch and C. A. Werner, *Biomaterials*, 2009, **30**, 5049–5060.
14 V. Guarino, M. A. Alvarez-Perez, A. Borriello, T. Napolitano and L. Ambrosio, *Adv. Healthcare Mater.*, 2013, **2**, 218–227.
15 K. Shah, D. Vasileva, A. Karadaghy and S. P. Zustiak, *J. Mater. Chem. B.*, 2015, **3**, 7950–7962.
16 M. Imaninezhad, Development of Hydrogel-Carbon Nanotube Composites and Templated Hydrogels for Neural Tissue Engineering Applications, PhD Thesis, Saint Louis University, 2017.
17 X. Liu, A. L. Miller, S. Park, B. E. Waletzki, Z. Zhou, A. Terzic and L. Lu, *ACS Appl. Mater. Interfaces*, 2017, **9**, 14677–14690.
18 J. Ramón-Azcón, S. Ahadian, M. Estili, X. Liang, S. Ostrovidov, H. Kaji, H. Shiku, M. Ramalingam, K. Nakajima and Y. Sakka, *Adv. Mater.*, 2013, **25**, 4028–4034.
19 S. Lee, W. Wang, J. Hwang, U. Namgung and K.-T. Min, *Proc. Natl. Acad. Sci.*, 2019, **116**, 16074–16079.
20 F. J. Mirza and S. Zahid, *Neurosci. Bull.*, 2018, **34**, 349–358.
21 M. Şen, K. Ino, H. Shiku and T. Matsue, *Lab Chip*, 2012, **12**, 4328–4335.
22 M. Şen, K. Ino, J. Ramón-Azcón, H. Shiku and T. Matsue, *Lab Chip*, 2013, **13**, 3650–3652.
23 A. Sikora, J. Ramón-Azcón, M. Sen, K. Kim, H. Nakazawa, M. Umetsu, I. Kumagai, H. Shiku, T. Matsue and W. Teizer, *Biomed. Microdevices*, 2015, **17**, 78.
24 M. Tessier-Lavigne and C. S. Goodman, *Science*, 1996, **274**, 1123–1133.
25 A. Solanki, S. T. D. Chueng, P. T. Yin, R. Kappera, M. Chhowalla and K. B. Lee, *Adv. Mater.*, 2013, **25**, 5477–5482.
26 Y.-S. Hsiao, C.-C. Lin, H.-J. Hsieh, S.-M. Tsai, C.-W. Kuo, C.-W. Chu and P. Chen, *Lab Chip*, 2011, **11**, 3674–3680.
27 A. Ferrari, M. Cecchini, A. Dhawan, S. Micera, I. Tonazzini, R. Stabile, D. Pisignano and F. Beltram, *Nano Lett.*, 2011, **11**, 505–511.
28 K. Kang, S. E. Choi, H. S. Jang, W. K. Cho, Y. Nam, I. S. Choi and J. S. Lee, *Angew. Chem., Int. Ed.*, 2012, **51**, 2855–2858.
29 U. A. Aregueta-Robles, P. J. Martens, L. A. Poole-Warren and R. A. Green, *Acta Biomater.*, 2019, **95**, 269–284.
30 W. Hällström, C. N. Prinz, D. Suyatin, L. Samuelson, L. Montelius and M. Kanje, *Langmuir*, 2009, **25**, 4343–4346.
31 T. Urisu, in *Optogenetics*, Springer, 2015, pp. 391–403.